Applied Thermal Engineering 162 (2019) 114228

Contents lists available at ScienceDirect

Applied Thermal Engineering

journal homepage: www.elsevier.com/locate/apthermeng

Numerical study on transport properties of the working mixtures for coal supercritical water gasification based power generation systems

Xueming Yang[a], Yiyu Feng[a], Jiangxin Xu[a], Jianghao Jin[a], Yuanbin Liu[b], Bingyang Cao[b,*]

[a] Department of Power Engineering, North China Electric Power University, Baoding 071003, China
[b] Key Laboratory for Thermal Science and Power Engineering of Ministry of Education, Department of Engineering Mechanics, Tsinghua University, Beijing 100084, China

HIGHLIGHTS

- Viscosity of the $H_2O/CO_2/H_2$ mixtures and H_2O/CO_2 mixtures is investigated.
- Predicted values by EMD method and theoretical models are compared.
- Self-diffusion coefficient, H-bond number and RDF are calculated.
- The breakdown of Stokes–Einstein relation is found and discussed.

GRAPHICAL ABSTRACT

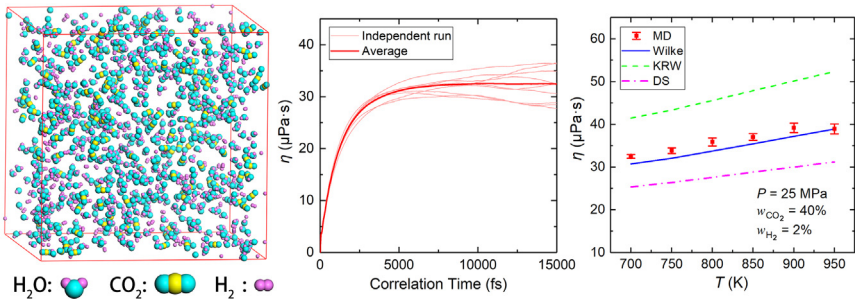

ARTICLE INFO

Keywords:
Viscosity
Coal supercritical water gasification
Molecular dynamics simulation
Mixtures
Local structures

ABSTRACT

Viscosity of $H_2O/CO_2/H_2$ mixtures or H_2O/CO_2 mixtures is a vital transport property and required in the design of equipment for coal supercritical water gasification based power generation systems, however, no experimental data and studies have examined these viscosities in supercritical regions of water. In this paper, viscosity of these mixtures in supercritical regions of water is investigated by molecular dynamics method and different theoretical models. Moreover, the self-diffusion coefficient, radial distribution functions and H-bond number are also calculated via molecular dynamics simulations to make a better understanding of the temperature dependences of the viscosity of the mixtures in supercritical regions of water at a molecular level. The breakdown of Stokes–Einstein relation for the $H_2O/CO_2/H_2$ mixture in supercritical regions of water is found and discussed. The prediction models and data put forth in this paper offer great value for practical application systems involving coal supercritical water gasification.

1. Introduction

Clean coal technologies, such as coal gasification, have been developed around the world to minimize environmental effects from coal utilization [1–3]. In recent years, coal supercritical water gasification technology and corresponding thermodynamics cycle power generation systems have received extensive attention [4–8]. With the technique of "boiling coal in water" proposed by Guo et al., [6] the organic matter of coal can be converted into gas (mainly H_2 and CO_2) while other elements (e.g., N, S, P, As and Hg) are deposited as inorganic salts. The two typical technology roadmaps [7,8] for the integrated thermodynamics cycle power generation systems based on coal supercritical water gasification are shown in Fig. 1. The production of the gasifier can be $H_2O/CO_2/H_2$ or H_2O/CO_2 mixtures in supercritical regions of water after separation and purification, and then they flow into the thermal power generation systems to generate electric power. This technology

* Corresponding author.
E-mail address: caoby@tsinghua.edu.cn (B. Cao).

https://doi.org/10.1016/j.applthermaleng.2019.114228
Received 21 April 2019; Received in revised form 28 June 2019; Accepted 7 August 2019
Available online 08 August 2019
1359-4311/

Nomenclature

k_B	Boltzmann constant, 1.3806×10^{-23} J/K
P	system pressure, MPa
V	system volume, Å^3
T	system temperature, K
t	time, s
v_i	velocity of molecule i, m/s
m_i	mass of molecule i, kg
r_{ij}	distance between molecules (sites) i and j, Å
f_{ij}	force acting on molecule i due to interactions with molecule j, N
u_{ij}	interaction potential energy between molecules i and j, kJ/mol
q	atomic charge, e
x	mole fraction, unitless
w	mass fraction, unitless
M	molecular weight, g/mol
T_B	the boiling point at 1 atmosphere pressure, K
N_A	Avogadro constant, 6.02×10^{23} mol^{-1}
N	total molecular number in the system
C_{SE}	the Stokes-Einstein coefficient
D	the self-diffusion coefficient, m^2 s^{-1}
V_{vdW}	the van-der-Waals volume, L/mol
n_{OH}	H-bond number
R	the ideal gas constant, 8.314472 J/(K mol)

Greek symbols

ε_{ij}^{kl}	the LJ energy parameter, kcal/mol
σ_{ij}^{kl}	the LJ size parameter, Å
ε_0	the vacuum permittivity
η	viscosity, μPa s
ρ	density, kg/m^3

Subscript

i, j	refers to individual molecule i or j
α, β	the direction in Cartesian coordinates
m	refers to mixture
C	critical
R	reduced

Superscript

k, l	refers to individual site k or l
Sim	simulation data
Exp	experimental data
NIST	data from national institute of standards and technology

Abbreviation

MD	molecular dynamics
EMD	equilibrium molecular dynamics
RDF	the radial distribution function
NACF	stress–stress normalized autocorrelation function
LJ	Lennard-Jones
LAMMPS	large-scale atomic/molecular massively parallel simulator
PPPM	particle-particle/particle-mesh
KRW	Kestin-Ro-Wakeham model
DS	Dean-Stiel model
EH	Ely and Hanley model
NIST	national institute of standards and technology
NEMD	non-equilibrium molecular dynamics
ARD	absolute relative deviation
AARD	average absolute relative deviation
ARE	absolute relative error
AARE	average absolute relative error
MSD	the mean square displacement

has many advantages, such as no pollutants, zero net CO_2 emissions, and high coal-electricity efficiency [7].

The thermophysical properties of $H_2O/CO_2/H_2$ or H_2O/CO_2 mixtures should be understood in the design and analysis of the coal supercritical water gasification based thermodynamics cycle power generation systems [9–11]. Among the thermophysical properties, viscosity is one of the most important transport properties for the fluids. However, so far there is no report or data available for the viscosity for $H_2O/CO_2/H_2$ mixtures and H_2O/CO_2 mixtures in supercritical regions of water, and it is fairly difficult and challenging to be obtained accurately under high-temperature extreme conditions via experimental measurements [12].

Molecular dynamics (MD) simulation has been proved to be an effective theoretical way of studying the viscosity of fluids. Liang et al. [13] employed an ab initio potential model to predicted shear viscosity of CO_2 gas without using any experimental data at the pressure of 1 atm and temperature range of 300–1000 K; the maximum error of simulation results compared with experiment data was 1.82%. Medina et al. [14] carried out equilibrium molecular dynamics (EMD) simulations for liquid water at temperatures in the range of 273–368 K. They found that the viscosity obtained by the flexible SPC/Fw model agrees with experimental data better than that by the rigid SPC/E model. Nieszporeket al. [15] calculated the viscosity of aqueous sodium perchlorate solution. The average error of viscosity obtained using TIP4P/2005 water model was 9.0% compared with experiment data. Yu et al. [16] investigated the viscosity of SiO_2/H_2O solid-gas system using EMD simulations with three different SiO_2/H_2O models. In many recent studies for the thermal energy storage and concentrating solar power applications [17–19], the viscosity of the melts or the nanofluids are also investigated via MD simulations. Ding et al. [17] performed MD simulations on viscosity of molten alkali carbonate K_2CO_3, and they found the simulation results are reasonable and reliable with an overall error of 12.05% compared with experimental data. Aguilar et al. [19] investigated the viscosity of NiO-based nanofluids with different nanoparticle mass concentrations for concentrating solar power applications. Besides the MD simulation method, some empirical theoretical models [20–24] for evaluating the viscosities of the mixtures may be another alternative, however most of these models are developed based on experimental data of common gases and their prediction reliability for water based mixtures in supercritical regions of water are still unknown.

In this paper, the viscosity of $H_2O/CO_2/H_2$ mixtures and H_2O/CO_2 mixtures in supercritical regions of water is predicted using EMD simulations and theoretical models. The radial distribution function (RDF) and the hydrogen bonds (H-bond) are calculated and analyzed for the local structure and viscosity of the water-based mixtures. The MSD and the self-diffusion coefficient are also computed via MD simulations. To allow readers to compare the obtained calculations, all numerical data and uncertainty estimates are provided in the Data in Brief.

2. Methodology

2.1. Green–Kubo formula

In this work, the viscosity is calculated by the Green–Kubo formulas and the EMD simulations:

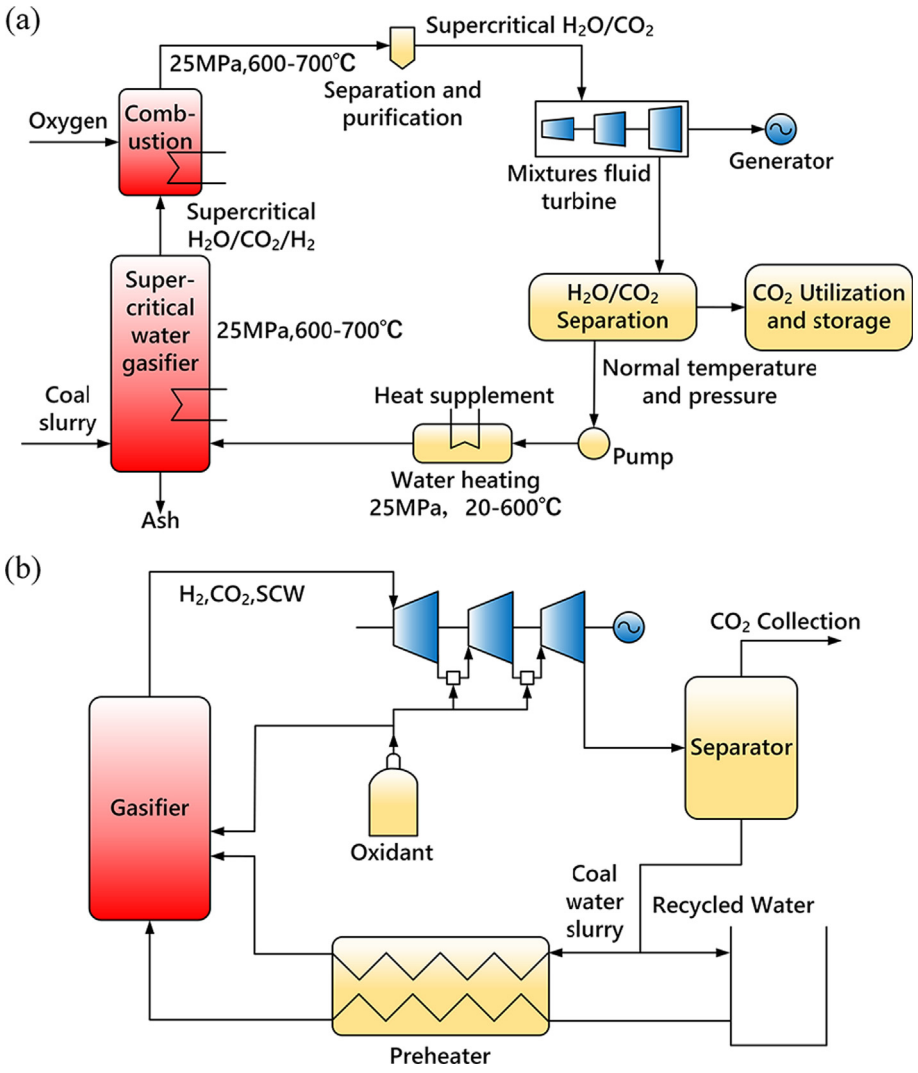

Fig. 1. Schematic diagram of the integrated thermodynamics cycle power generation systems based on coal supercritical water gasification. (a) Reproduced from Ref. [8]; (b) reproduced from Ref. [7].

$$\eta = \frac{V}{3k_B T}\int_0^\infty \sum_\alpha \sum_\beta \langle P_{\alpha\beta}(0)P_{\alpha\beta}(t)\rangle \mathrm{d}t \tag{1}$$

where η is the shear viscosity, V and T denote the volume and the temperature of the system. k_B is the Boltzmann constant equal $1.3806504 \times 10^{-23}$ J/K. α and β denote the x, y and z direction in Cartesian coordinates ($\alpha \neq \beta$). The angle bracket $\langle\rangle$ denotes the average of the autocorrelation function. $P_{\alpha\beta}(t)$ is the components of the pressure tensor of $\alpha\beta$ direction at time t which can be calculated as follows [13]:

$$P_{\alpha\beta}(t) = \frac{1}{V}\left[\sum_{i=1}^{N} m_i v_{i\alpha} v_{i\beta} + \sum_{i=1}^{N-1}\sum_{j>i}^{N} r_{ij\alpha} f_{ij\beta}\right] \tag{2}$$

where N is the number of molecules, m_i is the mass of molecule i. $v_{i\alpha}$ and $v_{i\beta}$ is velocity component of molecule i at α and β direction, while r and f correspond to the displacement and force between two molecules, respectively.

2.2. Potentials for molecular dynamics simulation

In this study, the combined Lennard-Jones (LJ) and Coulomb potential is adopted:

$$u_{ij} = \sum_{k=1}^{m}\sum_{l=1}^{n}\left\{4\varepsilon_{ij}^{kl}\left[\left(\frac{\sigma_{ij}^{kl}}{r_{ij}^{kl}}\right)^{12} - \left(\frac{\sigma_{ij}^{kl}}{r_{ij}^{kl}}\right)^{6}\right] + \frac{q_i^k q_j^l}{4\pi\varepsilon_0 r_{ij}^{kl}}\right\} \tag{3}$$

where u_{ij} is the interaction energy between molecule i and molecule j, $\varepsilon_{ij}^{kl}$is the LJ energy parameter, σ_{ij}^{kl} is the LJ size parameter, r_{ij}^{kl} is the distance between sites k and l, q_i^k is the charge on site sites k of molecule i, and ε_0 is the vacuum permittivity.

To choose appropriate force field models for pure H_2O, CO_2, H_2, and their mixtures, 11 force fields models are examined, including SPC/E model [25], TIP4P model [26], TIP4P/2005 model [27], SPC/Fd model [28] and SPC/Fw model [28] for pure H_2O, EPM model [29], EPM2 model [29], MSM3 model [30], Cygan model [31], and TraPPE model [32] for CO_2, and the two-site model [33] for H_2. The force field parameters of the models are listed in Table 1. To describe the interactions between unlike atoms in the system, the interaction parameters of the potential are obtained via the Lorentz-Berthelot mixing rule [34] which is the most commonly used combining rule [35].

2.3. Molecular simulation details

The LAMMPS software package [36] is used to perform our EMD simulations. The simulations are conducted in a three-dimensional cubic box with periodic boundary conditions in all directions. The long-

Table 1
Force field parameters of the models used in this work.

Molecule	Model	Site	q (e)	σ(Å)	d_{OM} (Å)	ε (kcal/mol)
H_2O	SPC/E	O	−0.8476	3.166	—	0.1553
		H	0.4238	—	—	—
	TIP4P	O	—	3.1536	—	0.155
		H	0.52	—	—	—
		M	−1.04	—	0.15	—
	TIP4P/2005	O	—	3.1589	—	0.1852
		H	0.5564	—	—	—
		M	−1.1128	—	0.1546	—
	SPC/Fw	O	−0.82	3.1654	—	0.1554
		H	0.41	—	—	—
	SPC/Fd	O	−0.82	3.1654	—	0.1554
		H	0.41	—	—	—
CO_2	EPM	C	0.6645	2.785	—	0.0576
		O	−0.33225	3.064	—	0.1651
	EPM2	C	0.6512	2.757	—	0.0559
		O	−0.3256	3.033	—	0.1602
	MSM3	C	0.594	2.785	—	0.0576
		O	−0.297	3.014	—	0.1651
	TraPPE	C	0.7	2.8	—	0.0537
		O	−0.35	3.05	—	0.1572
	Cygan	C	0.6512	2.8	—	0.05600
		O	−0.3256	3.028	—	0.15995
H_2	Two-site	H	—	2.72	—	0.0199

range electrostatic interactions are computed with the particle–particle particle-mesh (PPPM) method [37] with a cutoff distance of 13 Å and an accuracy of 10^{-4} in force. For LJ interactions, a cutoff distance of 13 Å is used. The time step is set as 0.4 fs for the pure fluid and the mixtures. In the simulations, the simulations initially run in NVT ensemble to equilibrate the system at a given temperature for 1 ns, then switch to the NPT ensemble if needed to control the pressure and equilibrate the system at a given pressure for another 1 ns. Finally, it is switched to the NVE ensemble, the first 1 ns are performed to relax the system, and next 2 ns or longer time are used to calculate the viscosity.

More details for the simulations can be found in Section 3, including the adopted force field models, and the simulation strategy adopted and the details of process of the EMD simulation for the pure fluids and the mixtures.

2.4. Theoretical models for the calculations of viscosity of the mixtures

The Wilke model [20], DS model [21], KRW model [22,23], and EH model [24] are commonly used in the evaluation of the viscosity of the gas mixtures [38,39]. However, there is no study for these models in the prediction of the viscosity of the H_2O/CO_2 binary mixtures and the ternary mixtures of $H_2O/H_2/CO_2$ because of the absence of experimental measurements. Here the EH model cannot be used for the H_2O/CO_2 binary mixtures and the ternary mixtures of $H_2O/H_2/CO_2$ due to the lack of the value of related binary interaction parameters from the experimental data in supercritical regions of water. Thus, the left three models are studied in this study.

The Wilke model to calculate the viscosity of mixtures is as follows [20]:

$$\eta = \sum_{i=1}^{n} \frac{\eta_i}{1 + \frac{1}{x_i}\sum_{j=1,j\neq i}^{n} x_j \phi_{ij}} \tag{4}$$

$$\phi_{ij} = \frac{[1 + (\eta_i/\eta_j)^{0.5}(M_j/M_i)^{0.25}]^2}{2\sqrt{2}\,[1 + (M_i/M_j)]^{0.5}} \tag{5}$$

where η is the calculated viscosity of the mixture, x_i, M_i, and η_i are mole fraction, molecular weight and viscosity of component i, respectively.

The equations of the DS model to calculate the viscosity of mixtures are as follows [21]:

$$(\eta - \eta^*)\xi = 10.8 \times 10^{-5}(e^{1.439\rho_R} - e^{-1.11\rho_R^{1.858}}) \tag{6}$$

$$\eta^*\xi = 166.8 \times 10^{-5}(0.1338T_R - 0.0932)^{5/9} \quad T_R \geqslant 1.5 \tag{7}$$

$$\eta^*\xi = 34.0 \times 10^{-5}T_R^{8/9} \quad T_R < 1.5 \tag{8}$$

$$\xi = \frac{T_{cm}^{1/6}}{(\sum_{i=1}^{n} x_i M_i)^{1/2} P_{cm}^{2/3}} \tag{9}$$

In the above equations, T_{cm} and P_{cm} represent critical temperature and critical pressure of mixture. T_R and ρ_R are reduced temperature and reduced density. η^* is the viscosity of mixtures at low pressures (< 5 bar).

$$P_{cm} = \sum_{i=1}^{n} x_i P_{ci} \tag{10}$$

$$T_R = T/T_{cm} \tag{11}$$

$$T_{cm} = \sum_{i=1}^{n} x_i T_{ci} \tag{12}$$

$$\rho_R = \rho_m/\rho_{cm} \tag{13}$$

$$\rho_{cm} = \frac{\sum_{i=1}^{n} x_i M_i}{\sum_{i=1}^{n} x_i V_{ci}} \tag{14}$$

where P_{ci}, T_{ci} and V_{ci} are critical pressure, critical temperature and critical volume of component i, respectively. ρ_{cm} and ρ_m are critical density and density of mixtures.

The equations of the KRW model to calculate the viscosity of mixtures are as follows [22,23]:

$$\eta = \frac{\begin{vmatrix} H_{11} & \cdots & H_{1n} & x_1 \\ H_{n1} & \cdots & H_{nn} & x_n \\ x_1 & \cdots & x_n & 0 \end{vmatrix}}{\begin{vmatrix} H_{11} & \cdots & H_{1n} \\ H_{n1} & \cdots & H_{nn} \end{vmatrix}} \tag{15}$$

$$H_{ii} = \frac{x_i^2}{\eta_i} + \sum_{\substack{k=1 \\ k\neq i}}^{n} \frac{2x_i x_k}{\eta_{ik}} \frac{M_i M_k}{(M_i + M_k)^2}\left(\frac{5}{3A_{ik}^*} + \frac{M_k}{M_i}\right) \tag{16}$$

$$H_{ij} = -\frac{2x_i x_j}{\eta_{ij}} \frac{M_i M_j}{(M_i + M_j)^2}\left(\frac{5}{3A_{ij}^*} - 1\right) \qquad i \neq j \tag{17}$$

In the equation, the interaction viscosity η_{ij} is given by

$$\eta_{ij} = \frac{5}{16}\left(\frac{k_B M_{ij} T}{\pi N_A}\right)^{\frac{1}{2}} \frac{1}{\sigma_{ij}^2 \Omega_{22}} \tag{18}$$

$$M_{ij} = \frac{2M_i M_j}{M_i + M_j} \tag{19}$$

where k_B and N_A are Boltzmann constant and Avogadro constant, respectively. $A^* = \Omega_{22}/\Omega_{11}$. Ω_{11} and Ω_{22} can be calculated by the formula as follows.

$$In\Omega_{22} = 0.45677 - 0.53955(InT^*) + 0.18265(InT^*)^2 - 0.03629(InT^*)^3 + 0.00241(InT^*)^4 \qquad 1 < T^* < 90 \tag{20}$$

$$In\Omega_{11} = 0.347 - 0.444(InT^*) + 0.093(InT^*)^2 - 0.010(InT^*)^3 \qquad 0.5 < T^* < 25 \tag{21}$$

where $T^* = k_B T/\varepsilon_{ij}$. The energy and length scaling parameters, σ_{ij} and ε_{ij}, are given as [40]

$$\sigma_{ij} = (1 - k_{ij,\sigma})\sqrt{\sigma_j \sigma_i} \tag{22}$$

$$\varepsilon_{ij}/k_B = (1 - k_{ij,\varepsilon})\sqrt{(\varepsilon_i/k_B)(\varepsilon_j/k_B)} \tag{23}$$

where $k_{ij,\sigma}$ and $k_{ij,\varepsilon}$ are the binary interaction parameters which obtained by fitting experimental data.

3. Results and discussion

3.1. Predicting viscosity using EMD simulation

The uncertainties of the viscosity results for different independent runs of EMD simulations are generally rather large. To solve this problem, statistics from several independent runs are necessary to obtain a reliable value result of the viscosity [41]. Besides, appropriate correlation time and enough long simulation time for the EMD simulations should be chosen carefully. In all the EMD simulations of this work, we perform ten independent simulations on pure fluid and mixtures by changing initial velocity. Finally, an average viscosity for the given temperature and pressure (or mass density) are evaluated by averaging over the values for the ten independent runs, and the error estimate is obtained by the standard error of the values for each independent run.

To choose the correlation time, the stress–stress normalized autocorrelation function (NACF) is calculated for the pure H_2O, CO_2, H_2 and their mixtures. Fig. 2 shows the NACF for the pure H_2O, CO_2, H_2 with different force field models. The NACF are calculated at temperature of 750 K and mass density of 100 kg/m^3 for the pure H_2O and pure CO_2, and temperature of 750 K and mass density of 5 kg/m^3 for the pure H_2. The calculated NACF for different force field models for pure water is shown in Fig. 2(a). It can be observed that the NACF decays relatively fast to zero in about 5000 fs. However, for the carbon dioxide force field models, it takes long correlation times (about 8000 fs or more dependent on the force field model adopted) to sufficiently converge the NACF, as shown in Fig. 2(b). For the pure H_2, correlation time about 6000 fs is needed for the convergence of NACF to zero, as shown in Fig. 2(c).

In fact, the following two points should be considered when determine the duration of the correlation time windows τ: (1) The correlation time used to calculate the NACF should be long enough to capture its full decay; (2) longer correlation times will have larger statistical uncertainty because less data are available for its calculation. Therefore, in this work, we choose the value of τ in simulations while NACF fully decay and almost converge to zero.

For example, with the Cygan force field model, the calculated viscosity corresponding to the correlation time for the pure CO_2 at temperature of 750 K and mass density of 200 kg/m^3 is shown in Fig. 3(a). The calculated viscosity by EMD simulations converges at 36.4 μPa s which is very close to theη^{NIST} = 37.1 μPa s (data from NIST database). In fact, the value of τ is also dependent on the state of the mixtures. As shown in Fig. 3(b), with the decrease of the mass density ρ, the correlation time needed increases steadily for NACF fully decay to zero and the convergence of the viscosity.

3.2. System size

Here we need to examine the effect of the system size in the simulations. EMD simulations with different system sizes, the total molecular number N = 1000, 2000, 3000, 4000, and 5000, are carried out for the $H_2O/CO_2/H_2$ mixtures (w_{H_2} = 2%, w_{CO_2} = 40%) at pressure of 25 MPa and temperature of 700 K. For example, Fig. 4(a) shows the simulation model for system with N = 1000; the calculated viscosity corresponding to the correlation time for ten independent runs and their average is shown Fig. 4(b). To obtain the final result, we take the converged value of the averaged viscosity. The predicted results for different system sizes are shown in Fig. 5. Markers with error bars represent the average values and the corresponding standard errors for a given N. The solid line indicates the average over the five system sizes and the dashed lines indicate the corresponding standard error. It can be seen that the calculated viscosity using EMD is insensitive to system size. In fact, this is one of the main advantages of the EMD method for transport properties calculation compared to the Non-equilibrium molecular dynamics (NEMD) methods [42].

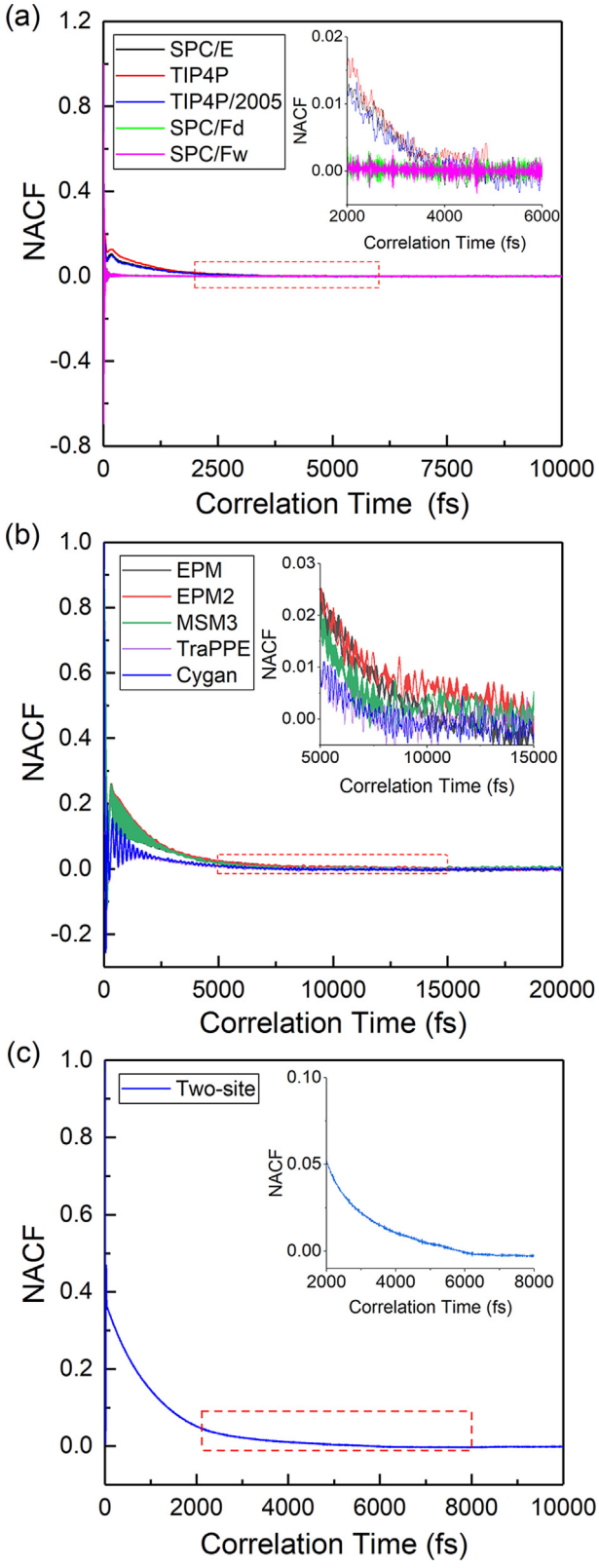

Fig. 2. The NACF calculated with different force field models: (a) H_2O; (b) CO_2; (c) H_2.

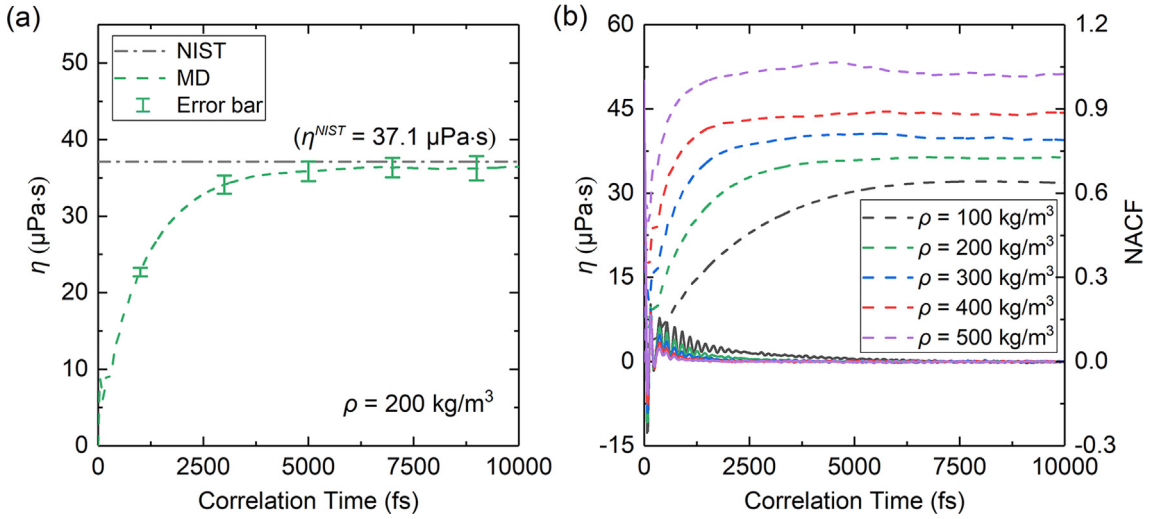

Fig. 3. (a) Viscosity as a function of correlation time for the pure CO_2 at temperature of 750 K and mass density of 200 kg/m^3; (b) NACF and viscosities as a function of correlation time for the pure CO_2 with different mass densities.

3.3. Pure fluid

Due to the absence of experimental data related to the viscosity of H_2O/H_2 binary mixtures, H_2O/CO_2 binary mixtures, and $H_2O/CO_2/H_2$ ternary mixtures in supercritical regions of water, the correct selection of force fields must be obtained by comparing data from the National Institute of Standards and Technology (NIST) with simulation results of pure fluids. In fact, many studies [43–48] have taken NIST viscosity data of pure CO_2, H_2O, and H_2 as referents because they are relatively accurate and publicly available. In this article, viscosity data of pure H_2O, CO_2, and H_2 from the NIST database are used as referents for calculations in EMD simulations.

First, the viscosity of pure H_2O and pure CO_2 is calculated using EMD simulations at a temperature of 750 K and mass density ranging from 100 to 500 kg/m^3 using different force field models; results are illustrated in Fig. 6a and c, respectively. The viscosity of pure H_2 is calculated using EMD simulations at a temperature of 750 K and mass density ranging from 5 to 20 kg/m^3, as shown in Fig. 6e. Then, to examine viscosity variations with temperature at a given pressure, the viscosity of pure H_2O, pure CO_2, and pure H_2 is calculated through EMD simulations at a pressure of 25 MPa and temperature range of 700 to 950 K, as indicated in Fig. 6b, d, and f, respectively. NIST data are also presented in Fig. 6 for comparison with the simulation results.

To clarify the comparison and discussion, the absolute relative

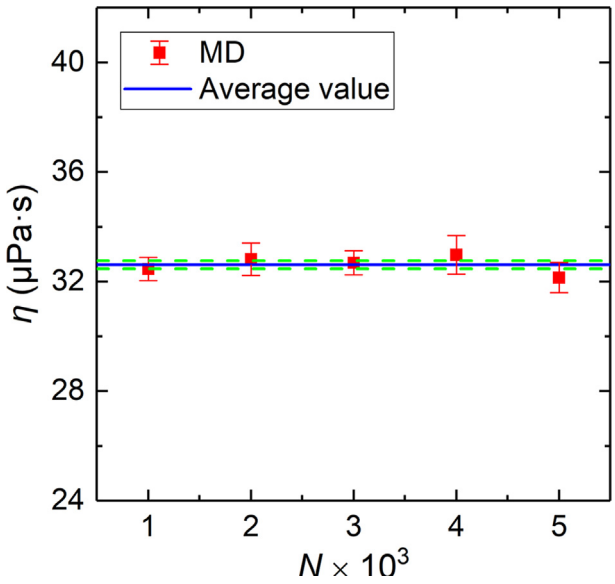

Fig. 5. Viscosity calculated by EMD simulation for $H_2O/H_2/CO_2$ mixtures with different system sizes.

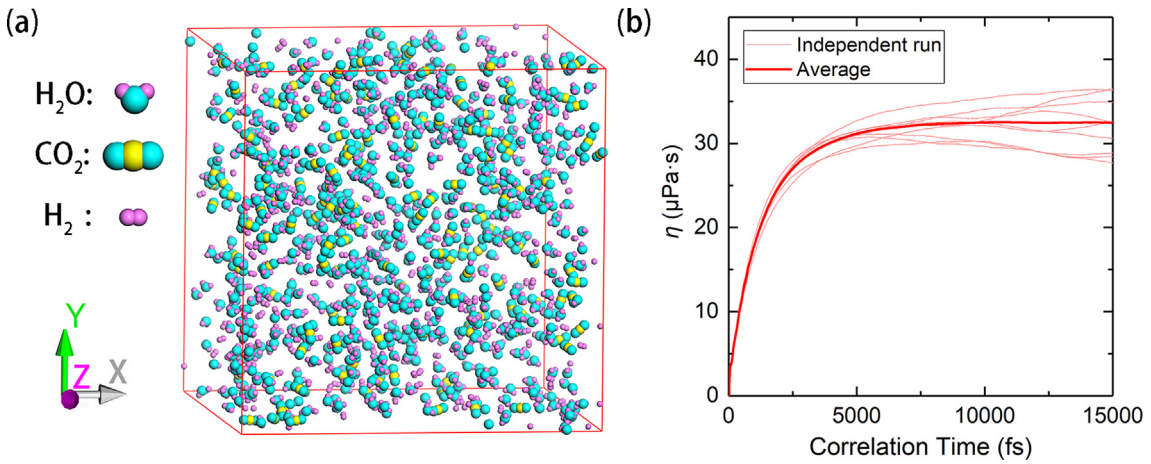

Fig. 4. (a) Simulation system for $H_2O/H_2/CO_2$ mixtures with total molecular number N = 1000; (b) Calculated viscosity as a function of correlation time by ten independent runs and their average.

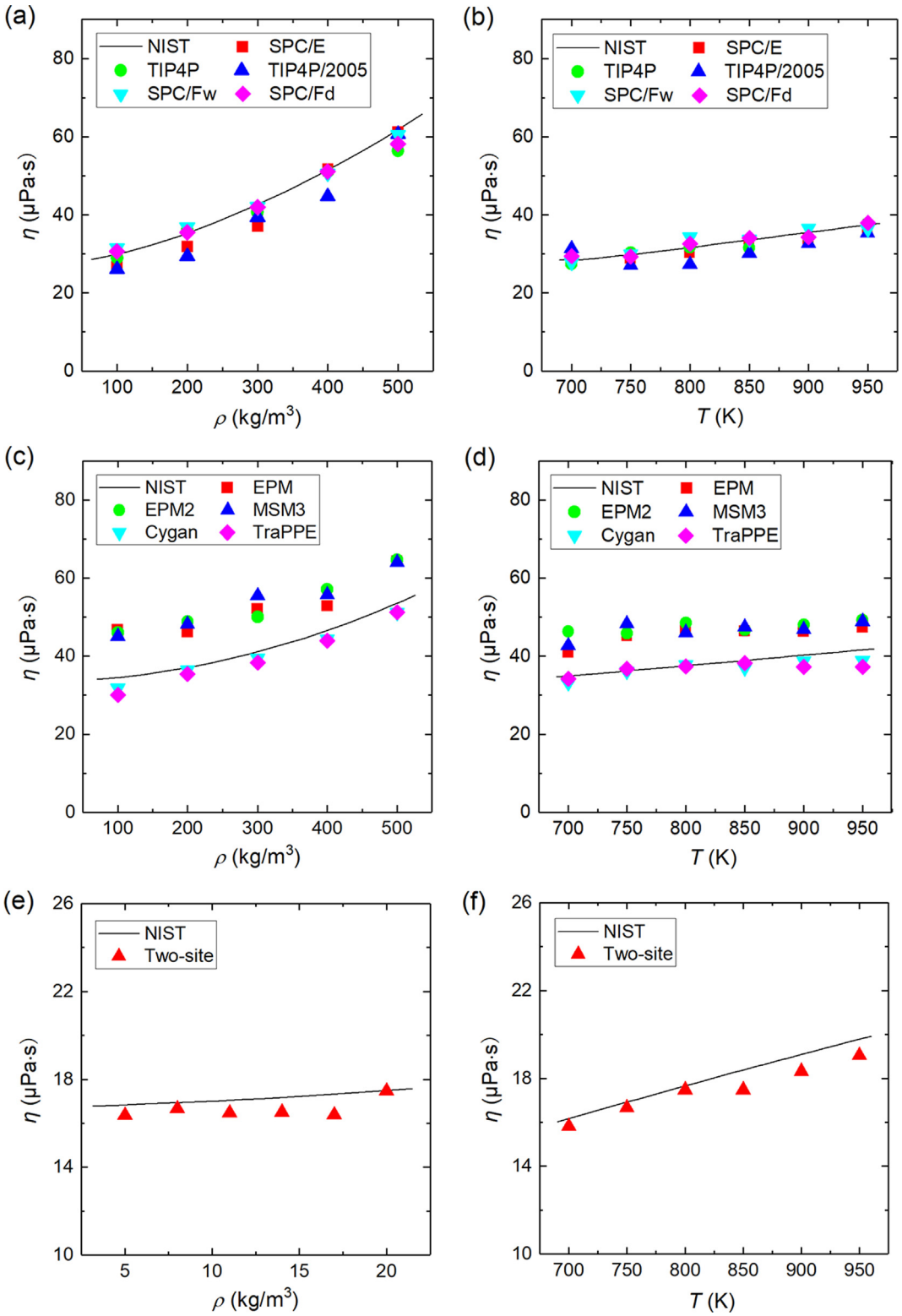

Fig. 6. The viscosity as a function of the mass density and temperature calculated by EMD simulation with different force field models. (a) and (b): H_2O; (c) and (d): CO_2; (e) and (f): H_2.

errors (AREs) between MD simulation results and NIST data (or experimental data) are calculated as $ARE = |\eta^{sim} - \eta^{NIST}|/\eta^{NIST} \times 100\%$ (or $ARE = |\eta^{sim} - \eta^{EXP}|/\eta^{EXP} \times 100\%$), where η^{sim}, η^{NIST}, and η^{EXP} respectively denote the viscosity values from MD simulations, the NIST database and experiments. ARE results appear in Fig. 7 with corresponding data listed in Tables S2–S7 of the Data in Brief. The average absolute relative error (AARE) of the SPC/Fw model is smallest in the force field models for pure water, with a value of 2.31%. Among the force field models for pure CO_2, the Cygan models exhibit the best accuracy with AARE value of 4.08%. The AARE of the two-site model for pure H_2 is 2.52%, indicating that the two-site model can accurately describe the viscosity of hydrogen gas. Given the above simulations, we

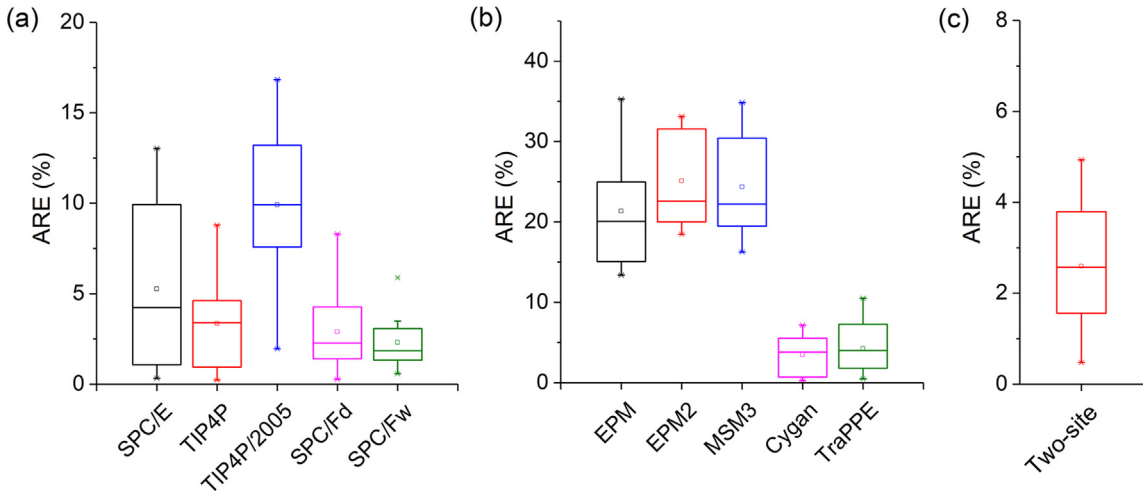

Fig. 7. AREs of viscosity calculated by EMD simulation with different force field models. (a) H_2O; (b) CO_2; (c) H_2.

recommend the SPC/Fw model for water molecules, Cygan model for carbon dioxide molecules, and two-site model for hydrogen molecules when predicting the viscosity of their mixtures.

3.4. Model validation with experimental data

No previous data are available pertaining to the viscosity of CO_2/H_2 binary mixtures, H_2O/H_2 binary mixtures, or $H_2O/CO_2/H_2$ ternary mixtures in supercritical regions of water; only experimental data [49] of CO_2/H_2 binary mixtures at lower pressures can be found. To validate the simulation method and force field models adopted in this paper, we calculate the viscosity of CO_2/H_2 binary mixtures and compare the simulation results with experimental data from Mal'tsev et al. [49] A longer production time (approximately 8 ns) in the EMD simulation is needed due to the prolonged correlation time (about 6 ns) to sufficiently converge the NACF for the CO_2/H_2 binary mixtures at lower pressures. Fig. 8 depicts the results for the viscosity of CO_2/H_2 binary mixtures at a pressure of 0.3 MPa and respective temperatures of 500 K, 800 K, and 1100 K. The predicted values of the theoretical models are also provided for comparison. Corresponding data are listed in Tables S8 and S9 of the Data in Brief, including the AAREs of the MD simulation and theoretical models when compared with the experimental data.

The AARE of the Wilke model is smallest, with a value of 3%, and that of the MD simulations is 6.51%. Here, the MD method does not exhibit better performance than the Wilke model in predicting the viscosity of CO_2/H_2 binary mixtures at relatively low pressure, but the predictive accuracy of the MD simulations is better than that of the KRW model (AARE = 10.43%) and DS model (AARE = 10.75%). This suggests that the results of the presented EMD model are acceptable.

Additionally, in the above calculations, the predictive accuracy of the models is shown in the following order: the MS model, EMD model, KRW model, and DS model; however, such a conclusion is only obtained for CO_2/H_2 mixtures at relatively low pressure. How it will be for CO_2/H_2 mixtures, H_2O/H_2 binary mixtures, and $H_2O/CO_2/H_2$ ternary mixtures at temperatures and pressures in supercritical regions of water remains unknown.

3.5. H_2O/CO_2 binary mixtures

No experimental data, simulation results, or NIST data are available regarding the viscosity of H_2O/CO_2 binary mixtures in supercritical regions. Thus, we compare our simulation results with those of theoretical models in the following states at different pressures (P), temperatures (T), mass densities (ρ), and mass fractions: (1) P = 25 MPa, T = 700–950 K, w_{CO_2} = 20%; (2) P = 25 MPa, T = 700–950 K, w_{CO_2} = 40%; (3) ρ = 100 kg/m^3, T = 700–950 K, w_{CO_2} = 20%; (4) ρ = 100 kg/m^3, T = 700–950 K, w_{CO_2} = 40%. Results are shown in Fig. 9a–d. To clarify the comparison, the absolute relative deviations (ARDs) between the MD simulation results and calculation results using theoretical models are calculated as follows:

$$\mathrm{ARD} = \left| \frac{\eta^{sim} - \eta^{calc}}{\eta^{sim}} \right| \times 100\% \tag{24}$$

where $\eta^{sim}$is the viscosity calculated from the MD simulations, and η^{calc} is the value calculated using the theoretical models. The data in Fig. 9 and the corresponding ARDs are provided in Tables S10–S13 of the Data in Brief. The averaged ARDs (AARDs) are respectively 6.93%,

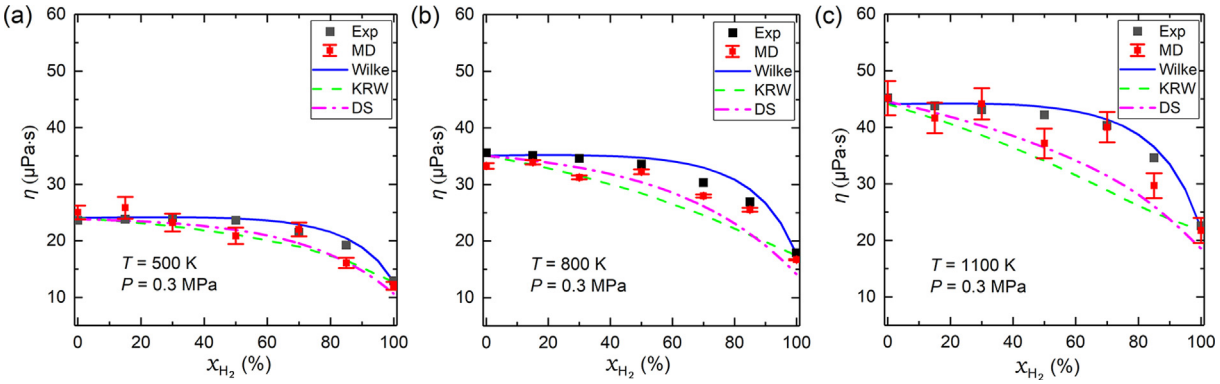

Fig. 8. Viscosity as a function of the mole fraction of H_2 (x_{H_2}) at a pressure (P) of 0.3 MPa for CO_2/H_2 binary mixtures. (a) T = 500 K; (b) T = 800 K; (c)T = 1100 K.

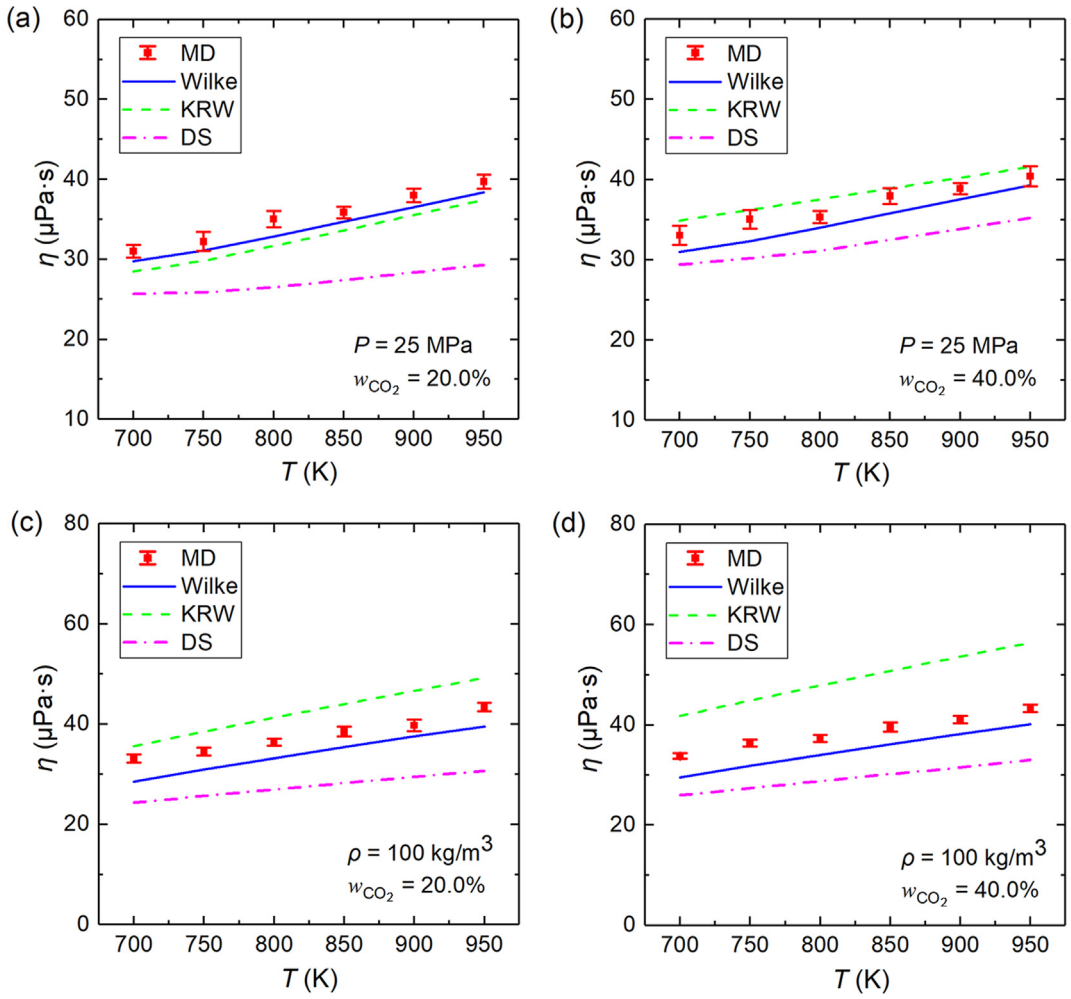

Fig. 9. Viscosity calculated by EMD simulation and the theoretical models for H_2O/CO_2 mixtures.

12.90%, and 21.43% for the Wilke model, KRW model, and DS model.

Fig. 10 describes the viscosity variation of H_2O/CO_2 mixtures with different w_{CO_2} atρ = 100 kg/m^3 and a temperature of 750 K. Data and accompanying ARDs are provided in Tables S14–S15 of the Data in Brief. According to the statistics, the overall AARDs for the Wilke model, KRW model, and DS model are 3.82%, 29.95%, and 12.77%, respectively; hence, the prediction results of the Wilke model and EMD simulations are comparable, but deviations in the KRW model and the DS model when compared with EMD simulations are relatively large.

3.6. $H_2O/CO_2/H_2$ ternary mixtures

For $H_2O/CO_2/H_2$ ternary mixtures, EMD simulations are carried out and findings are compared with theoretical models in the following states: (1) P = 25 MPa, T = 700–950 K, w_{H_2} = 1%, w_{CO_2} = 20%; (2) P = 25 MPa, T = 700–950 K, w_{H_2} = 2%, w_{CO_2} = 40%; (3) ρ = 100 kg/m^3, T = 700–950 K, w_{H_2} = 1%, w_{CO_2} = 20%; (4) ρ = 100 kg/m^3, T = 700–950 K, w_{H_2} = 2%, w_{CO_2} = 40%. Fig. 11a–d indicate the results; data and ARDs appear in Tables S16–S19 of the Data in Brief. The overall AARDs are respectively 3.77%, 24.72%, and 22.92% for the Wilke model, KRW model, and DS model.

Fig. 12 indicates the viscosity variation in $H_2O/H_2/CO_2$ mixtures with different w_{CO_2} at ρ = 100 kg/m^3 and 750 K; refer to Tables S20–S21 of the Data in Brief for detailed data and ARDs. The AARDs for the Wilke model, KRW model, and DS model are 8.88%, 24.62%, and 15.27%, respectively. Overall, when predicting the viscosity of $H_2O/H_2/CO_2$ mixtures, the AARD of the Wilke model is smallest and that of the KRW model is largest.

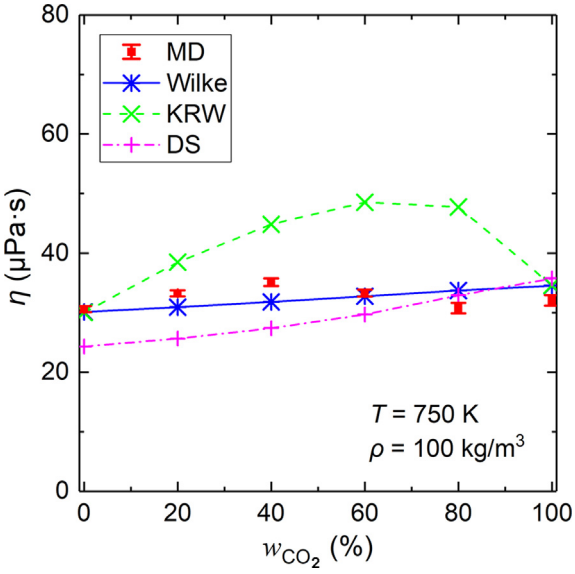

Fig. 10. Viscosity as a function of w_{CO_2} calculated by EMD simulation and the theoretical models for H_2O/CO_2 mixtures.

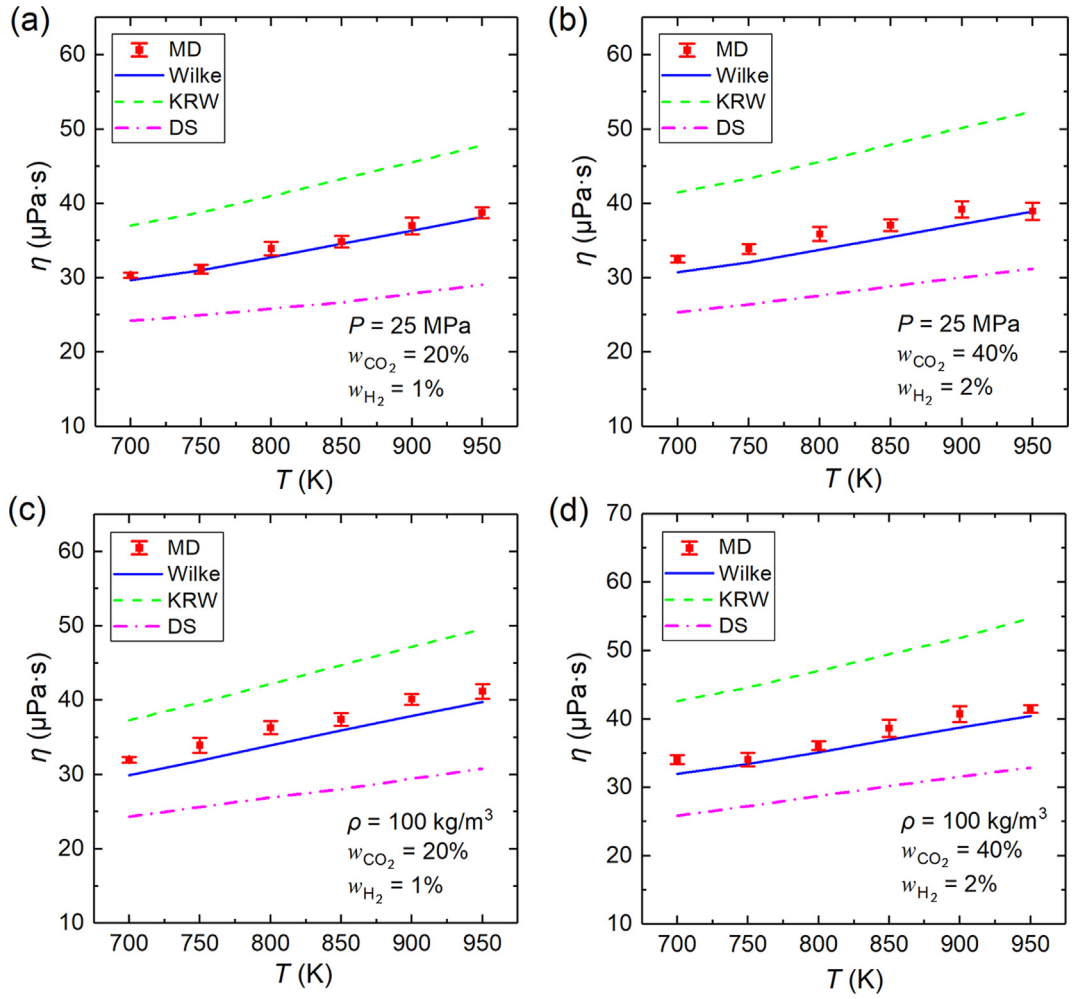

Fig. 11. Viscosity as a function of temperature calculated by EMD simulation and the theoretical models for $H_2O/H_2/CO_2$ mixtures.

3.7. Discussion

From the above calculations, we have provided an EMD simulation model and calculation data for the viscosity of H_2O/CO_2 mixtures and $H_2O/H_2/CO_2$ mixtures in supercritical regions of water in the absence of experimental data. Since the validity and accuracy of the adopted MD method has been demonstrated in predicting the viscosity of pure H_2O, pure H_2, pure CO_2, and CO_2/H_2 mixtures. Thus, the MD simulation results can serve as a reference to choose the theoretical models in the absence of experimental data. By comparing the EMD simulation model with the theoretical models, the AARD of the Wilke model is smallest among all models.

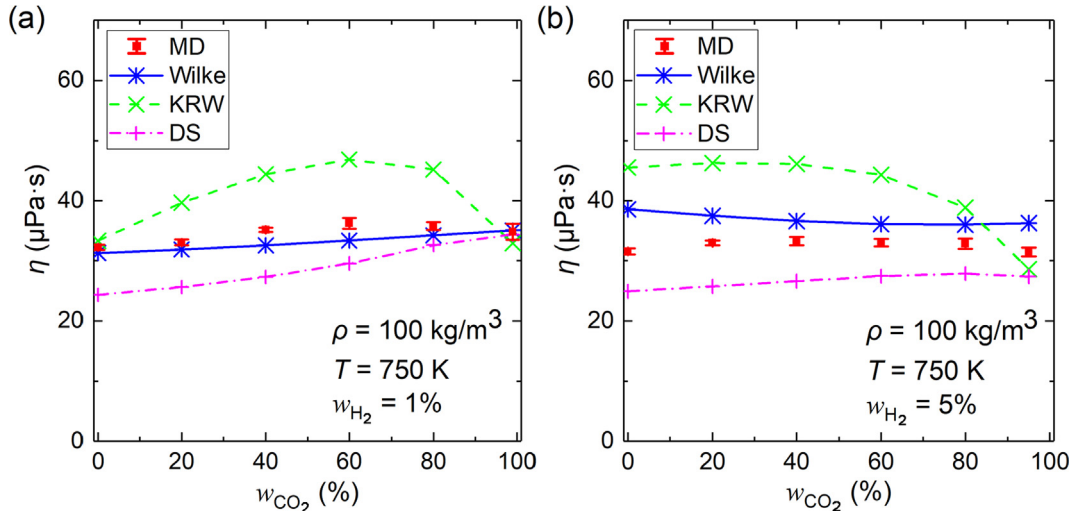

Fig. 12. Viscosity as a function of w_{CO_2} calculated by EMD simulation and the theoretical models for $H_2O/H_2/CO_2$ mixtures.

For the Wilke model, component viscosity is used to predict the viscosity of the mixtures, and in our work the viscosity of pure H_2O, pure H_2, and pure CO_2 are obtained directly from the NIST database, which is close to the experimental data. In fact, Wilke [20] has stated that this model can provide satisfactory prediction on multicomponent systems if the viscosities of pure components of the mixtures are accurate at a given temperature and pressure. Moreover, Tan et al. [38] reported that the Wilke model has an AARE of 2.0% for viscosity of CO_2/N_2 and $CO_2/N_2/Ar$ mixtures at different working conditions compared to experimental data. All these indicate that the Wilke model can provide acceptable predictions.

In the KRW model, the viscosity prediction depends heavily on binary interaction parameters in the model. Unfortunately, in predicting the viscosity of H_2O/CO_2 mixtures and $H_2O/H_2/CO_2$ mixtures, the binary interaction parameters $k_{ij,\sigma}$ and $k_{ij,\varepsilon}$ for H_2O/H_2 and H_2O/CO_2 are not available when using this model due to a lack of experimental data; these parameters are therefore set to zero in accordance with the suggestion in Ref [38], resulting in poor predictive accuracy. The DS model is empirical and does not require binary interaction parameters for gas pairs and the component viscosities as input. However, as pointed out by Tan et al. [38], Eqs. (7) and (8) in the DS model were developed based on data for pure argon or other nonpolar substances via regression. To achieve a more accurate prediction, a regression curve should be developed based on experimental data of the H_2O/CO_2 and $H_2O/H_2/CO_2$ mixtures. Based on the above comparisons and discussion, the Wilke model can be recommended to predict the viscosity of H_2O/CO_2 mixtures and $H_2O/H_2/CO_2$ mixtures among all tested theoretical models.

3.8. Structure analysis

In both water and water-based mixtures, the hydrogen bonds (H-bond) affect the transportation properties [50–52]. However, It is still quite challenging to evaluate the H-bond effect on the viscosity of the water-based mixtures quantitatively, and the H-bond effect on the viscosity of the supercritical water is still unknown. Here we calculate the radial distribution function (RDF) of the $H_2O/H_2/CO_2$ ternary mixtures for the MD simulations in the following two states: (1) P = 25 MPa, T = 700–950 K, w_{H_2} = 1%, w_{CO_2} = 20%; (2) ρ = 100 kg/m^3, T = 700–950 K, w_{H_2} = 1%, w_{CO_2} = 20%, as shown in Fig. 13(a) and (b). The total RDF (g(r)$_{total}$) is the weighted sum of g(r) for all the different atom pairs. In Fig. 13(b) and (c), the $g(r)_{O(H_2O)-H(H_2O)}$ for this two conditions are provided to describe the O-H distances for neighboring H_2O molecules, and the first peaks locates at about 2.0 Å, which are shorter than the sum of Van der Waals radii of the oxygen and hydrogen atoms of 2.7 Å. With the increase of the temperature, the amplitude of the peaks for $g(r)_{O(H_2O)-H(H_2O)}$ decrease gradually, and the first peaks of $g(r)_{O(H_2O)-H(H_2O)}$ even becomes an insignificant shoulder at its place. These indicate that the size of small clusters and the average number of H-bonds per molecule decrease with increasing temperature.

H-bond can be defined by geometric conditions and energy conditions [53]: (1) $R(O\cdot\cdot H) \leqslant 2.41$Å; (2) $\theta(O-H\cdot\cdot O) \geqslant 130°$; (3) an interaction energy between the hydrogen bonded water molecules to be more negative than −12.9 kJ/mol (symbol $\cdot\cdot$ indicates the H-bond between different water molecules, while symbol − indicates the Hydroxide inside the water molecule). To evaluate the H-bond effect quantitatively, the H-bond number is calculated via MD simulation. As shown in Fig. 14(a) and (b), the average H-bond number n_{OH} for both pure water and $H_2O/H_2/CO_2$ ternary mixtures in supercritical regions

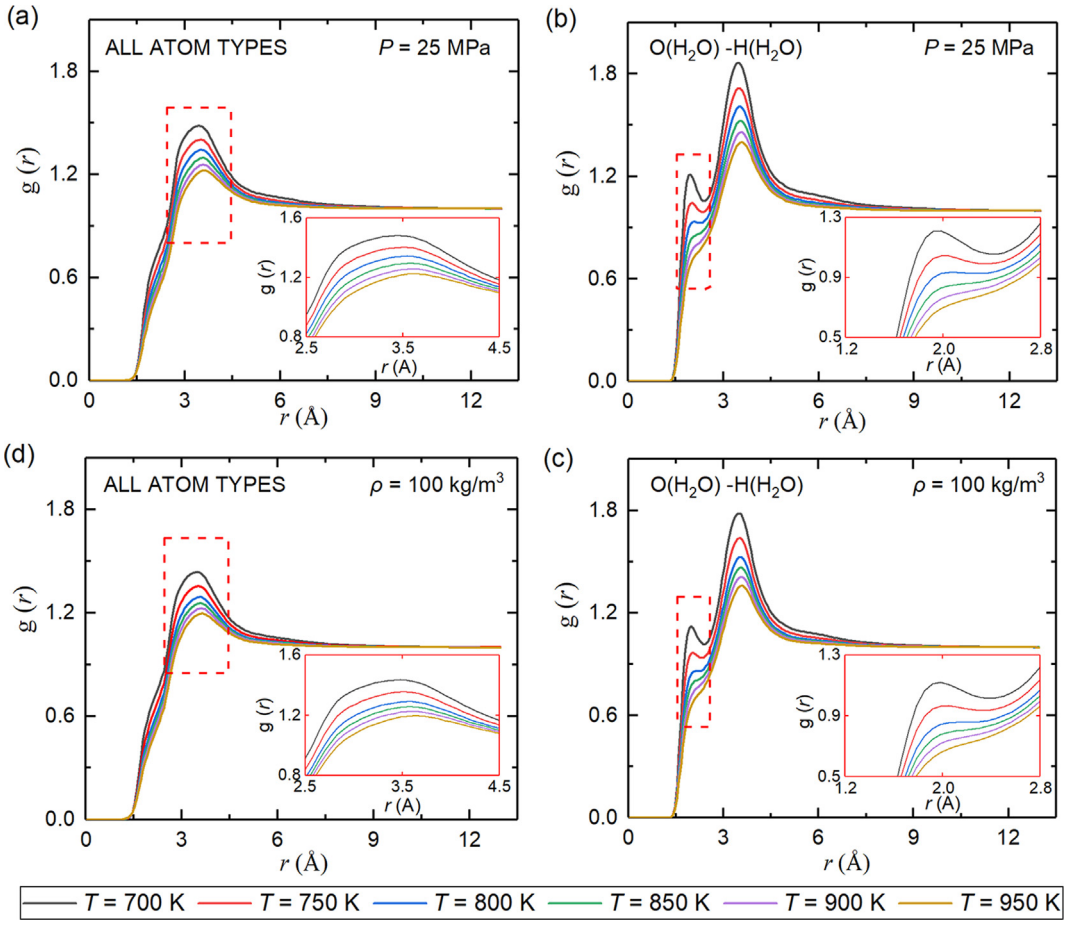

Fig. 13. RDF between different atom types for $H_2O/H_2/CO_2$ mixtures: (a) All atom types; (b) $O(H_2O)$-$H(H_2O)$. (w_{H_2} = 1%, w_{CO_2} = 20%, P = 25 MPa).

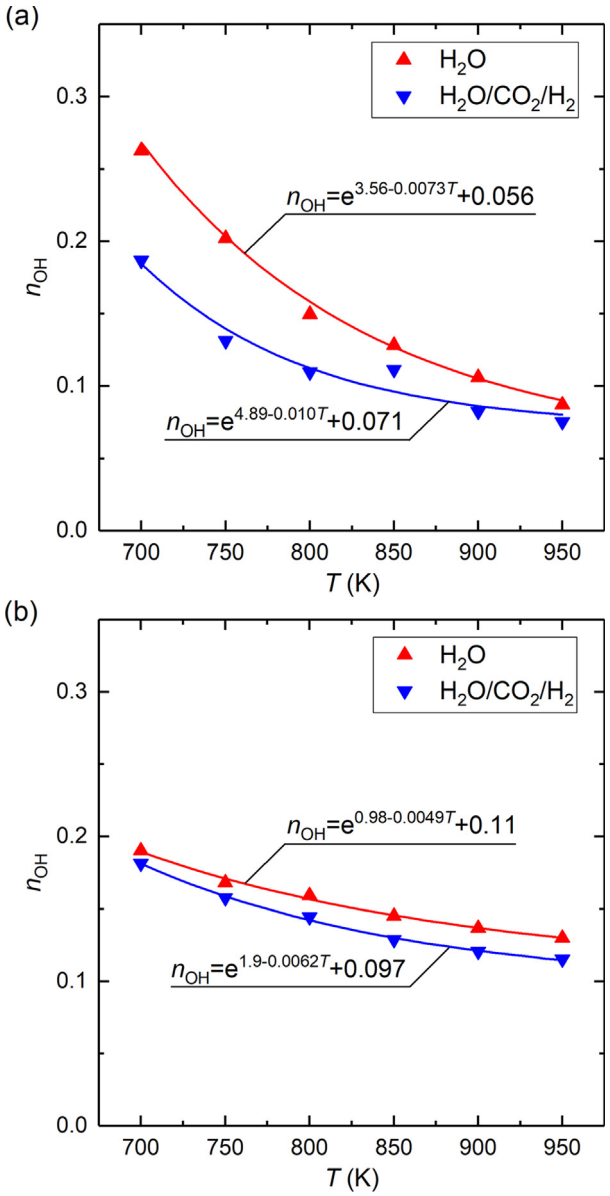

Fig. 14. The average H-bond number n_{OH} as a function of temperature for both pure water and $H_2O/H_2/CO_2$ ternary mixtures in supercritical regions of water. (a) $P = 25$ MPa; (b) $\rho = 100\ kg/m^3$.

decreases exponentially with the temperature. Such a trend of exponential decay of n_{OH} with the temperature for SCW agrees well with those reported data by Mizan et al. [54].

When only considering pure water in supercritical region and following the idea of Marcus [50], we can obtain the relationship between the viscosity and H-bond number for supercritical water ($P = 25$ MPa, $T = 700$–950 K; or $\rho = 100\ kg/m^3$, $T = 700$–950 K) by regression analysis as follows:

$$\log(\eta)(\mu Pa{\cdot}s) = 6.02\left(1 - \frac{V_{vdW}}{V_m}\right) - 20298.51\frac{1}{RT} + 5.12n_{OH} \tag{25}$$

where V_{vdW} is the van-der-Waals volume, V_m is the molar volume, R is the ideal gas constant and equals to 8.314472 J/(K mol). The value of the V_{vdW} can be obtained from DIPPR database [55] and equals 12.4 cm^3/mol. This equation can well explain the increasing trend of viscosity of the supercritical water with the increasing temperature shown in Fig. 6(b). However, it is still quite challenging to evaluate the H-bond effect on the viscosity of the water-based mixtures quantitatively because how to obtain the van-der-Waals volume V_{vdW} or the intrinsic volume of the mixtures is still questionable. Thus further investigation will be conducted on this issue in our future work.

Moreover, the Stokes–Einstein equation has been extensively used to calculate or estimate the viscosity of different fluids under ambient conditions. However, it may break down in the estimation of the viscosity for $H_2O/H_2/CO_2$ ternary mixtures in supercritical regions.

The Stokes–Einstein equation describes the relationship between the self-diffusion coefficient and viscosity as follows:

$$D\eta/T = \frac{2k_B}{\pi C_{SE}\sigma} \tag{26}$$

where σ is the hydrodynamic diameter and C_{SE} is the Stokes-Einstein coefficient. As is well known, $C_{SE} = 6$ for the stick boundary condition and$C_{SE} = 4$ for the slip boundary condition.

The self-diffusion coefficient D can be obtained from the mean square displacement (MSD):

$$D = \frac{1}{6}\lim_{t\to\infty}\frac{d}{dt}\left\langle \frac{1}{N}\sum_{i=1}^{N}[r_i(0) - r_i(t)]^2 \right\rangle \tag{27}$$

where $r_i(t)$ and $r_i(0)$ are the position of i^{th} molecule at time t and 0. The part inside the angle brackets denotes an average of MSD.

The MSD of $H_2O/CO_2/H_2$ mixture with$w_{H_2} = 1\%$ and$w_{CO_2} = 20\%$ is predicted with MD method for the two conditions: $P = 25$ MPa, $T = 700$–950 K; (2) $\rho = 100\ kg/m^3$, $T = 700$–950 K, as shown in Fig. 15(a) and (c). By using Eq. (27), the self-diffusion coefficient D is calculated from the MSD values, as shown in Fig. 15(b) and (d). It can be observed that the self-diffusion coefficient D almost increase lineally with the increasing temperature.

The Stokes–Einstein relation states that $D\eta/T$ is a constant and is independent of the external conditions. However, studies [56,57] have shown the breakdown of Stokes–Einstein relation in the supercooled liquids or supercritical water. Here we calculated the $D\eta/T$ for the $H_2O/CO_2/H_2$ mixture ($w_{H_2} = 1\%$ and$w_{CO_2} = 20\%$), as shown in Fig. 16. We find that it doesn't obey the Stokes–Einstein relation. In $H_2O/CO_2/H_2$ mixtures at the studied conditions, $D\eta/T$increases lineally with the increasing of the temperature. Therefore we can conclude that it is not suitable to predict the viscosity of $H_2O/CO_2/H_2$ mixtures or H_2O/CO_2 mixtures by directly using the Stokes–Einstein relation.

4. Conclusions

The viscosity of H_2O/CO_2 and $H_2O/CO_2/H_2$ mixtures is one of the key transport properties in design and optimization of the equipments in thermodynamics cycle power generation system based on coal supercritical water gasification. In this paper, the viscosity properties of the H_2O/CO_2 binary mixture and $H_2O/CO_2/H_2$ mixtures in supercritical regions of water are investigated via EMD simulations and theoretical methods. Simulation models for predicting viscosity of the mixtures are validated, and force models and simulation strategy are recommended. Comparisons show that the prediction results of the Wilke model agree well with the MD simulations.

The RDF and the hydrogen bonds are calculated and analyzed for the local structure and viscosity of the water-based mixtures. The MSD and the self-diffusion coefficient are also computed via MD simulations, and the breakdown of the Stokes–Einstein relation in $H_2O/CO_2/H_2$ mixtures in supercritical regions of water is found and discussed. Results in this paper could offer references for the design and optimization of a thermodynamic system based on coal supercritical water gasification.

Declaration of Competing Interest

The authors declare no competing financial interest.

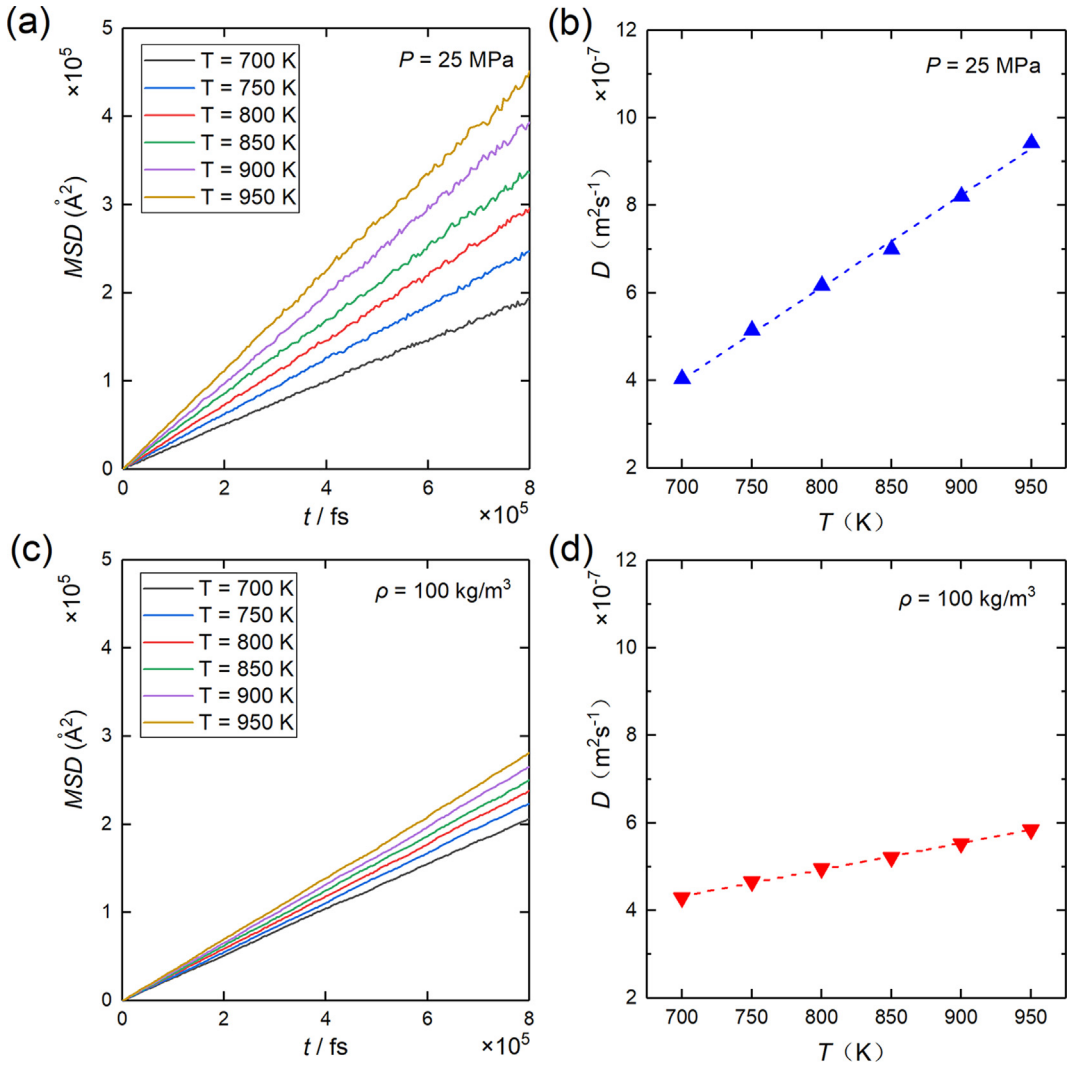

Fig. 15. The MSD and the self-diffusion coefficient $D$of $H_2O/CO_2/H_2$ mixtures(w_{H_2} = 1% andw_{CO_2} = 20%).

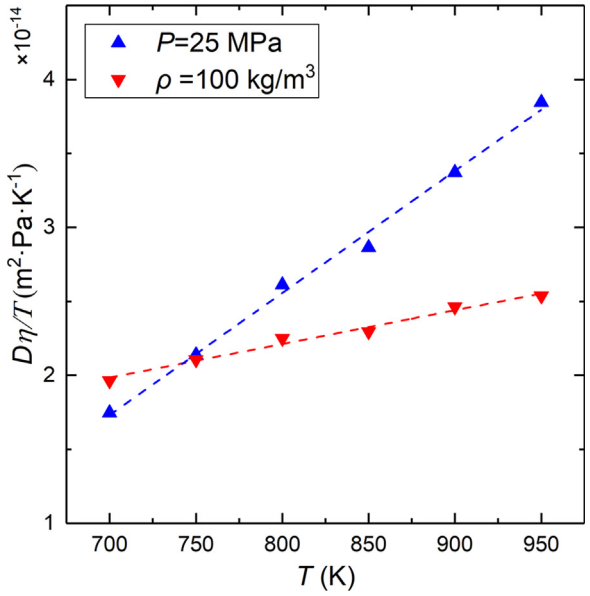

Fig. 16. The calculated $D\eta/T$ for the $H_2O/CO_2/H_2$ mixture (w_{H_2} = 1% and w_{CO_2} = 20%).

Acknowledgments

This work was supported by the National Key R&D Program of china (Grant No. 2016YFB0600100) and the Natural Science Foundation of Hebei Province of China (Grant No. E2019502138).

References

[1] K.P. Keboletse, T. Mongalenyane, L. Kelebopile, P. Oladijo, S. Kutua, Investigating the suitability of Morupule coal for coal gasification technology, MRS Adv. 3 (38) (2018) 2235–2245.
[2] L. Wang, Y. Jia, S. Kumar, R. Li, R.B. Mahar, M. Ali, K. Memon, Numerical analysis on the influential factors of coal gasification performance in two-stage entrained flow gasifier, Appl. Therm. Eng. 112 (2017) 1601–1611.
[3] Y. Zhao, B. Yu, B. Wang, S. Zhang, Y. Xiao, Heat integration and optimization of direct-fired supercritical CO_2 power cycle coupled to coal gasification process, Appl. Therm. Eng. 130 (2018) 1022–1032.
[4] Z. Chen, X. Zhang, L. Gao, S. Li, Thermal analysis of supercritical water gasification of coal for power generation with partial heat recovery, Appl. Therm. Eng. 111 (2017) 1287–1295.
[5] Z. Chen, X. Zhang, W. Han, L. Gao, S. Li, Exergy analysis on the process with integrated supercritical water gasification of coal and syngas separation, Appl. Therm. Eng. 128 (2018) 1003–1008.
[6] L. Guo, H. Jin, Boiling coal in water: hydrogen production and power generation system with zero net CO_2 emission based on coal and supercritical water gasification, Int. J. Hydrogen Energy 38 (29) (2013) 12953–12967.
[7] L. Guo, H. Jin, Y. Lu, Supercritical water gasification research and development in China, J. Supercrit. Fluid 96 (2015) 144–150.
[8] L. Guo, L. Zhao, Y. Lu, H. Jin, Hydrogen production and the integrated thermodynamics cycle power generation systems based on coal supercritical water

gasification, J. Eng. Therm. 03 (2017) 228–229.
[9] X. Yang, J. Xu, S. Wu, M. Yu, B. Hu, B. Cao, et al., A molecular dynamics simulation study of PVT properties for $H_2O/H_2/CO_2$ mixtures in near-critical and supercritical regions of water, Int. J. Hydrogen Energy 43 (24) (2018) 10980–10990.
[10] S. Cheng, F. Shang, W. Ma, H. Jin, N. Sakoda, X. Zhang, et al., Density data of two (H_2 + CO_2) mixtures and a (H_2 + CO_2 + CH_4) mixture by a modified Burnett method at temperature 673 K and pressures up to 25 Mpa, J. Chem. Eng. Data (2019).
[11] X. Yang, C. Duan, J. Xu, Y. Liu, B. Cao, A numerical study on the thermal conductivity of $H_2O/CO_2/H_2$ mixtures in supercritical regions of water for coal supercritical water gasification system, Int. J. Heat Mass Tran. 135 (2019) 413–424.
[12] S.T. Munkejord, M. Hammer, S.W. Løvseth, CO_2 transport: data and models–a review, Appl. Energy 169 (2016) 499–523.
[13] Z. Liang, H.L. Tsai, Prediction of the transport properties of a polyatomic gas, Fluid Phase Equilibr. 293 (2) (2010) 196–204.
[14] J.S. Medina, R. Prosmiti, P. Villarreal, G. Delgado-Barrio, G. Winter, B. González, et al., Molecular dynamics simulations of rigid and flexible water models: temperature dependence of viscosity, Chem. Phys. 388 (1–3) (2011) 9–18.
[15] K. Nieszporek, J. Nieszporek, M. Trojak, Calculations of shear viscosity, electric conductivity and diffusion coefficients of aqueous sodium perchlorate solutions from molecular dynamics simulations, Comput. Theor. Chem. 1090 (2016) 52–57.
[16] Y. Yu, Y. Tao, Y. He, Transport properties of SiO2/H2O solid-gas system for industrial flue gas: a molecular dynamics study, Int. J. Heat Mass Tran. 110 (2017) 723–729.
[17] J. Ding, L. Du, G. Pan, J. Lu, X. Wei, J. Li, et al., Molecular dynamics simulations of the local structures and thermodynamic properties on molten alkali carbonate K_2CO_3, Appl. Energy 220 (2018) 536–544.
[18] J. Wang, C.L. Liu, Temperature and composition dependences of shear viscosities for molten alkali metal chloride binary systems by molecular dynamics simulation, J. Mol. Liq. 273 (2019) 447–454.
[19] T. Aguilar, J. Navas, A. Sánchez-Coronilla, E.I. Martín, J.J. Gallardo, P. Martínez-Merino, et al., Investigation of enhanced thermal properties in NiO-based nanofluids for concentrating solar power applications: a molecular dynamics and experimental analysis, Appl. Energy 211 (2018) 677–688.
[20] C.R. Wilke, A viscosity equation for gas mixtures, J. Chem. Phys. 18 (4) (1950) 517–519.
[21] D.E. Dean, L.I. Stiel, The viscosity of nonpolar gas mixtures at moderate and high pressures, AIChE J. 11 (3) (1965) 526–532.
[22] J. Kestin, H.E. Khalifa, S.T. Ro, W.A. Wakeham, The viscosity and diffusion coefficients of eighteen binary gaseous systems, Phys. A 88 (2) (1977) 242–260.
[23] A. Boushehri, B. Najafi, Viscosity of nonpolar gases (quaternary mixtures), J. Chem. Eng. Data 24 (1) (1979) 24–25.
[24] J.F. Ely, H.J.M. Hanley, Prediction of transport properties. 1. Viscosity of fluids and mixtures, Ind. Eng. Chem. Fundam. 20 (4) (1981) 323–332.
[25] H.J.C. Berendsen, J.R. Grigera, T.P. Straatsma, The missing term in effective pair potentials, J. Phys. Chem. 91 (24) (1987) 6269–6271.
[26] W.L. Jorgensen, J. Chandrasekhar, J.D. Madura, R.W. Impey, M.L. Klein, Comparison of simple potential functions for simulating liquid water, J. Chem. Phys. 79 (2) (1983) 926–935.
[27] J.L.F. Abascal, C. Vega, A general purpose model for the condensed phases of water: TIP4P/2005, J. Chem. Phys. 123 (23) (2005) 234505.
[28] Y. Wu, H.L. Tepper, G.A. Voth, Flexible simple point-charge water model with improved liquid-state properties, J. Chem. Phys. 124 (2) (2006) 024503.
[29] J.G. Harris, K.H. Yung, Carbon dioxide's liquid-vapor coexistence curve and critical properties as predicted by a simple molecular model, J. Phys. Chem. 99 (31) (1995) 12021–12024.
[30] J. Brodholt, B. Wood, Molecular-dynamics simulations of the properties of CO_2-H_2O mixtures at high-pressures and temperatures, Am. Miner. 78 (5–6) (1993) 558–564.
[31] R.T. Cygan, V.N. Romanov, E.M. Myshakin, Molecular simulation of carbon dioxide capture by montmorillonite using an accurate and flexible force field, J. Phys. Chem. C 116 (24) (2012) 13079–13091.
[32] A. Liu, T.L. Beck, Vapor−liquid equilibria of binary and ternary mixtures containing methane, ethane, and carbon dioxide from Gibbs ensemble simulations, J. Phys. Chem. B 102 (39) (1998) 7627–7631.
[33] R.F. Cracknell, Molecular simulation of hydrogen adsorption in graphitic nanofibers, Phys. Chem. Chem. Phys. 3 (11) (2001) 2091–2097.
[34] M.P. Allen, D.J. Tildesley, Computer simulation of liquids, Oxford University Press, 1989.
[35] T. Akıner, H. Ertürk, K. Atalık, Prediction of Thermal Conductivity and Shear Viscosity of Water-Cu Nanofluids Using Equilibrium Molecular Dynamics, ASME 2013 International Mechanical Engineering Congress and Exposition. American Society of Mechanical Engineers, (2013).
[36] S. Plimpton, Fast parallel algorithms for short-range molecular dynamics, J. Comput. Phys. 117 (1) (1995) 1–19.
[37] M.S. Kelkar, J.L. Rafferty, E.J. Maginn, J.I. Siepmann, Prediction of viscosities and vapor–liquid equilibria for five polyhydric alcohols by molecular simulation, Fluid Phase Equilibr. 260 (2) (2007) 218–231.
[38] Y. Tan, W. Nookuea, H. Li, E. Thorin, J. Yan, Evaluation of viscosity and thermal conductivity models for CO_2 mixtures applied in CO_2 cryogenic process in carbon capture and storage (CCS), Appl. Therm. Eng. 123 (2017) 721–733.
[39] H. Ke, Y. He, Y. Liu, F. Cui, Mixture working gases in thermoacoustic engines for different applications, Int. J. Thermophys. 33 (7) (2012) 1143–1163.
[40] J.C. Chichester, M.L. Huber, Documentation and assessment of transport property model for mixtures implemented in NIST REFPROP (Version 8.0). US department of commerce technology administration, Nat. Instit. Stand. Technol. (2008).
[41] Z. Fan, L.F.C. Pereira, H.Q. Wang, J.C. Zheng, D. Donadio, A. Harju, Force and heat current formulas for many-body potentials in molecular dynamics simulations with applications to thermal conductivity calculations, Phys. Rev. B 92 (9) (2015) 094301.
[42] A.J.H. McGaughey, M. Kaviany, Thermal conductivity decomposition and analysis using molecular dynamics simulations. Part I. Lennard-Jones argon, Int. J. Heat Mass Tran. 47 (8–9) (2004) 1783–1798.
[43] X. Li, J. Tian, A. Mulero, Empirical correlation of the surface tension versus the viscosity for saturated normal liquids, Fluid Phase Equilibr. 352 (2013) 54–63.
[44] M. Zheng, J. Tian, Á. Mulero, New correlations between viscosity and surface tension for saturated normal fluids, Fluid Phase Equilibr. 360 (2013) 298–304.
[45] H. Loria, H. Motahhari, M.A. Satyro, H.W. Yarranton, Process simulation using the expanded fluid model for viscosity calculations, Chem. Eng. Res. Des. 92 (12) (2014) 3083–3095.
[46] C.G. Aimoli, E.J. Maginn, C.R. Abreu, Transport properties of carbon dioxide and methane from molecular dynamics simulations, J. Chem. Phys. 141 (13) (2014) 134101.
[47] E. Yusibani, Y. Nagahama, M. Kohno, Y. Takata, P.L. Woodfield, K. Shinzato, et al., A capillary tube viscometer designed for measurements of hydrogen gas viscosity at high pressure and high temperature, Int. J. Thermophys. 32 (6) (2011) 1111.
[48] J.W. Leachman, R.T. Jacobsen, S.G. Penoncello, M.L. Huber, Current status of transport properties of hydrogen, Int. J. Thermophys. 28 (3) (2007) 773–795.
[49] V.A. Mal'tsev, O.A. Nerushev, S.A. Novopashin, V.V. Radchenko, W.R. Licht, E.J. Miller, et al., Viscosity of H_2-CO_2 mixtures at (500, 800, and 1100) K, J. Chem. Eng. Data 49 (3) (2004) 684–687.
[50] Y. Marcus, On transport properties of hot liquid and supercritical water and their relationship to the hydrogen bonding, Fluid Phase Equilibr. 164 (1) (1999) 131–142.
[51] Y. Marcus, On the relationships between transport and thermodynamic properties of organic liquids at ambient conditions, Fluid Phase Equilibr. 154 (2) (1999) 311–321.
[52] H. Fang, K. Ni, J. Wu, J. Li, L. Huang, D. Reible, The effects of hydrogen bonding on the shear viscosity of liquid water, Int. J. Sedim. Res. 34 (1) (2019) 8–13.
[53] A.G. Kalinichev, Universality of hydrogen bond distributions in liquid and supercritical water, J. Mol. Liq. 241 (2017) 1038–1043.
[54] T.I. Mizan, P.E. Savage, R.M. Ziff, Comparison of rigid and flexible simple point charge water models at supercritical conditions, J. Comput. Chem. 17 (15) (1996) 1757–1770.
[55] Project 801, Evaluated Process Design Data, Public Release Documentation, Design Institute for Physical Properties (DIPPR), American Institute of Cheical Engineers (AIChE), 2006.
[56] P. Bordat, F. Affouard, M. Descamps, F. Müller-Plathe, The breakdown of the Stokes-Einstein relation in supercooled binary liquids, J. Phys.-Condens. Mat. 15 (32) (2003) 5397.
[57] W.J. Lamb, G.A. Hoffman, J. Jonas, Self-diffusion in compressed supercritical water, J. Chem. Phys. 74 (12) (1981) 6875–6880.